

Two CubeSats with Micro-Propulsion in the QB50 Satellite Network

P.P. Sundaramoorthy

Electronic Research Laboratory, Faculty of Electrical Engineering, Mathematics & Computer Science, Delft University of Technology
Mekelweg 4, 2628 CD Delft, The Netherlands; +31152786098
P.P.Sundaramoorthy@tudelft.nl

E. Gill

Chair of Space Systems Engineering, Faculty of Aerospace Engineering, Delft University of Technology
Kluyverweg 1, 2629 HS Delft, The Netherlands;
E.K.A.Gill@tudelft.nl

C.J.M. Verhoeven

Chair of Space Systems Engineering, Faculty of Aerospace Engineering, Delft University of Technology
Kluyverweg 1, 2629 HS Delft, The Netherlands;
C.J.M. Verhoeven@tudelft.nl

J. Bouwmeester

Chair of Space Systems Engineering, Faculty of Aerospace Engineering, Delft University of Technology
Kluyverweg 1, 2629 HS Delft, The Netherlands;
J.Bouwmeester@tudelft.nl

ABSTRACT

A network of small low-cost satellites is the only realistic option for multi-point in-situ measurements in the lower thermosphere. The QB50 program, an initiative of the von Karman Institute of Fluid Dynamics (VKI), aims to employ a network of 50 CubeSats built by universities to study the lower thermosphere (90-320 km). All 50 CubeSats will carry identical sensors and will be launched together from a single launch vehicle. QB50 will also study the re-entry process by measuring a number of critical parameters during re-entry.

The Delft University of Technology (TUDelft) intends to provide two satellites out of the 50 CubeSats in the QB50 network. This paper will discuss the preliminary orbit analysis of the QB50 satellites that will allow a first order evaluation of mission performance parameters like lifetime and coverage. The paper will subsequently look at the two satellites provided by TUDelft, each of which is equipped with a highly miniaturized propulsion system in addition to the science payload. This scenario is an excellent opportunity to demonstrate relative motion control between two CubeSats and elevate university CubeSats as serious contenders for significant science missions. A first analysis assesses the possibility of drag compensation and differential drag compensation using the TUDelft satellites with micro-propulsion.

INTRODUCTION

The number of space missions using multiple satellites has been increasing in recent times and concepts of distributed space missions involving hundreds to thousands of spacecraft are envisioned for scientific applications^{1,2}. Enabled and enhanced functionality and flexibility are among the key motivations for missions employing distributed space systems. Space missions using massively distributed satellites are especially promising for standardized miniature spacecraft like CubeSats that have a low development cost and short development time.

CubeSats are standardized miniature satellites measuring 10 x 10 x 10 cm and having a mass of about 1 kg. CubeSats have been developed primarily as an education tool and in recent years are being more and more exploited for military applications, commercial services and business³. The constraints of limited functionality imposed on CubeSats by virtue of their small size do not make them serious contenders for scientific missions. However, new application scenarios like distributed space missions and continued miniaturization of payload and subsystems are expected to enhance the scientific contribution of CubeSat missions. The QB50 programme is an excellent

opportunity to demonstrate relative motion control between two CubeSats and elevate university CubeSats as serious contenders for significant science missions.

This paper will discuss the preliminary orbit analysis of the QB50 satellites that will allow a first order evaluation of mission performance parameters like lifetime and coverage. The paper will subsequently look at the two satellites provided by TUDelft, each of which is equipped with a highly miniaturized propulsion system in addition to the science payload.

Simulation of the orbital evolution of these distributed satellites provides insight into the relative geometry and evolution of the distributed cluster in space and its temporal and spatial resolution and coverage. Orbital dynamics of the satellites, solar activity based on launch date, and influence of deployment strategy are investigated to evaluate mission performance parameters such as altitude decay, absolute and relative orbit development, and mission lifetime.

This is followed by an analysis of the added benefits of a pair of active satellites in a cluster of uncontrolled satellites. The advantages to the QB50 programme offered by a pair of satellites with a micro-propulsion system that can be accommodated in a CubeSat like the one proposed for Delfi-n3xt are identified and summarized.

QB50 PROGRAMME

The QB50 mission has the following the scientific objectives⁴ :

- to study in situ the temporal and spatial variations of a number of key parameters in the lower thermosphere at 100-350 km altitude with a network of about 50 CubeSats, and carrying identical sensors,
- to study the re-entry process by measuring a number of key parameters during re-entry and by comparing predicted and actual CubeSat trajectories and orbital lifetimes

Space agencies are currently not pursuing any multi-spacecraft network for in-situ measurements in the lower thermosphere as the cost of a network of many satellites built to industrial standards would be prohibitively high and thus not justifiable in view of the limited orbital lifetime. No other space network for in-situ atmospheric measurements has been carried out in the past or is currently planned for. A network of satellites for in-situ measurements in the lower thermosphere can only be realized by using low-cost satellites. Thus, CubeSats with their mass range of 1-3

kg are the only realistic option for realizing such a mission.

For the QB50 network, double-unit CubeSats (10x10x20 cm) are foreseen. All 50 CubeSats will be launched together on a single launch vehicle, a Russian Shtil-2.1, into a near-circular orbit at about 350km altitude and 79° inclination. Following separation and orbit injection, the CubeSat orbits will, due to atmospheric drag, gradually decay. Thus, progressively lower and lower layers of the thermosphere will be explored by the satellites. The initial orbital altitude will be selected such that the mission lifetime of individual CubeSats will be about three months. A total of 36 CubeSats are envisaged to be provided by European universities in 21 countries, 10 by universities in the U.S., two by universities in Canada and two by Japanese universities.

The low initial altitude of the QB50 mission presents the following uniqueness and advantages^{5,3}:

- An envisaged lifetime of around 3months, much less than the 25 years stipulated by international space law and regulations ,
- Higher data rate for given onboard power due to smaller communication range
- A less harmful radiation environment justifying the use of low-cost Commercial-off-The-Shelf (COTS) components

CubeSat reliability is not a prime concern as mission objective is not compromised even if a few CubeSats fail.

SIMULATION SETUP

The simulation framework for orbit propagation is outlined in Figure 1. The basic methods, assumptions, and initial conditions are summarized in this section. The simulation is based on a model of a cluster launch mechanism that can separate satellites from a reference satellite to establish a distributed cluster of satellites.

CubeSats are deployed with a standardized deployment mechanism called P-POD⁶ (Poly Picosat Orbital Deployer). The P-POD uses a spring mechanism to glide the CubeSats out with an exit velocity of around 1.6 m/s. This exit velocity can be adjusted by varying the spring characteristics. To cover a broad range of typical exit velocities, we investigate test cases in which the separation model provides velocity increments between 1 m/s and 5 m/s. Further, we investigate the orbital evolution of the cluster through velocity increments in six different limiting directions around the reference satellite (positive and negative

along-track, cross-track and radial directions with respect to the reference satellite).

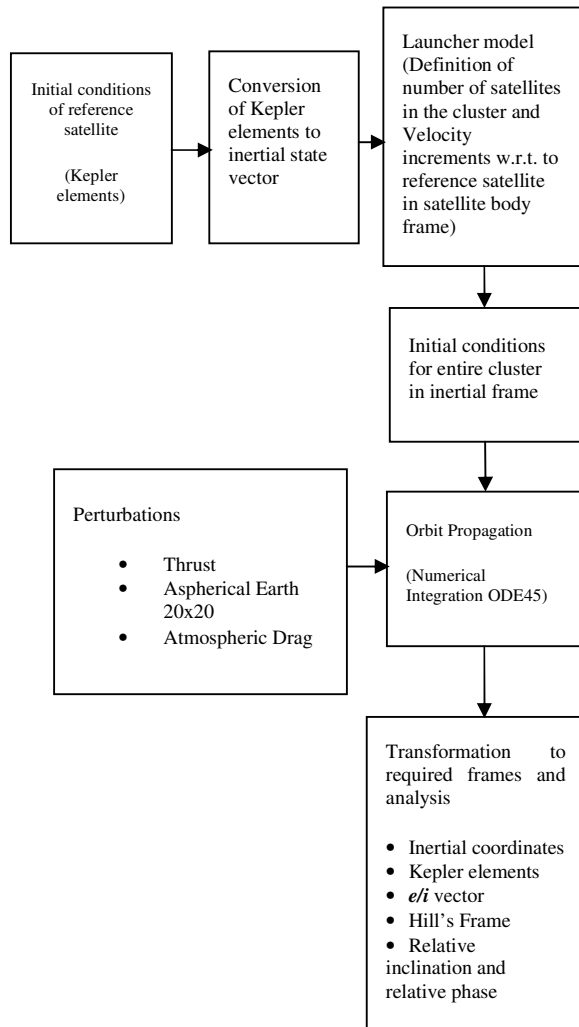


Figure 1: Basic Framework of Orbit Propagation Software

Table 1: Simulation approach

Integration	ODE45 (Matlab) RelTol 10^{-13} AbsTol 10^{-6}
Reference system	True of Date
Central body	Earth
Gravity Field	JGM3 up to 20x20
Third body	None
Non-conservative forces	Drag
Atmospheric Density	MSIS – 86
Drag Coefficient, C_D	2.2
Spacecraft Model	Cannon ball
Average area of cross section	0.021 m^2
Mass	2 kg
Attitude control	None
Solar array	Body Fixed
Number of satellites	Variable up to 50
Duration of simulation	Until Decay

Table 2: Initial Epoch and Kepler elements of Reference Satellite

Semi-major axis a	6678.1 km (300 km altitude)
Eccentricity e	0
Inclination i	79°
Right ascension of ascending node Ω	0°
Argument of perigee ω	0°
Mean anomaly at epoch	0°
Epoch	January 1 st 2013 00:00:00 UTC

The distance between satellites that are separated from a deployment mechanism in space can vary from millimeters to thousands of kilometers over the mission lifetime. The problem, therefore, cannot be categorized

into either the domain of close satellite formations or conventional satellite constellations. To analyze this orbital evolution and influence of perturbations, different representation schemes are employed like the Hill's frame, eccentricity-inclination vectors⁷, analemmas with relative phase and relative inclination⁸. In this paper only the Hill's frame is discussed in detail.

QB50 MISSION LIFETIME

A number of parameters influence the orbital lifetime of the QB50 satellites, like spacecraft mass, size, and shape; initial orbit of the satellites; solar activity during mission duration; and attitude of the satellites.

The launch date is significant primarily due to the solar cycle which leads to a time dependent variation in the atmospheric density. Consequently, atmospheric drag varies which influences the orbital decay and hence lifetime of the satellites. To identify and characterize this influence, the satellite orbits are propagated from an initial reference position shown in Table 2 for different levels of solar activity and varying spacecraft area of cross-section. Equation (1) gives the expression for the acceleration due to drag a_D ⁹.

$$a_D = \frac{1}{2} \rho C_D \left(\frac{A}{m} \right) v^2 \quad (1)$$

C_D is the drag coefficient, A is the cross-sectional area of the spacecraft perpendicular to the direction of motion and m is the mass of the satellite. ρ is the atmospheric density and v is the satellite velocity with respect to the atmosphere. Table 1 lists some of the assumptions made for simulating the orbits in the presence of drag. An average A of 0.021 m^2 derived by assuming a body fixed solar array on a 2-unit CubeSat ($20 \times 10 \times 10 \text{ cm}$), is adopted to simplify the analysis. This average area is used to approximate the box-model of the 2-unit CubeSat with a cannon-ball for simulation.

Spacecraft Cross-section

The influence of spacecraft area of cross-section on lifetime under different conditions of solar flux can be seen in Figures 2-4. Table 3 lists the orbital lifetime of the satellites for different conditions of solar flux and spacecraft area of cross-section. As extreme cases, it can vary from 85 days (solar minimum, minimum area of cross-section) to eight days (solar maximum, maximum area of cross-section).

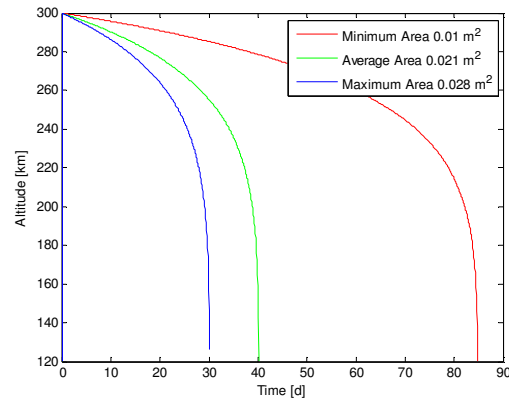


Figure 2: Influence of area of cross-section of the spacecraft on lifetime during solar minimum

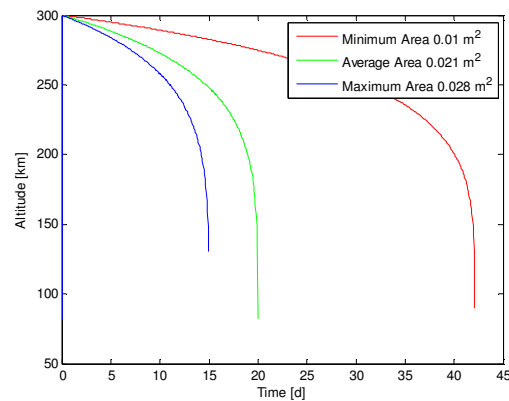


Figure 3: Influence of Area of cross-section of the spacecraft on lifetime during solar mean

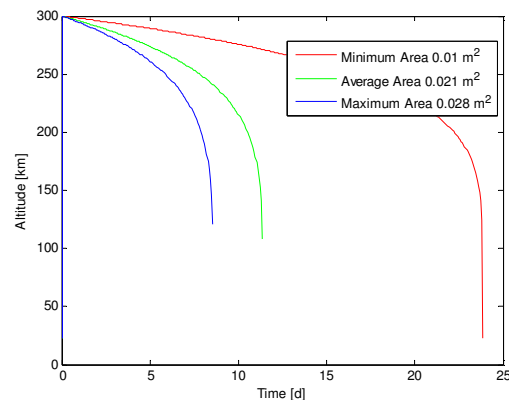


Figure 4: Influence of area of cross-section of the spacecraft on lifetime during solar maximum

Table 3: Time to decay under varying conditions of solar flux and spacecraft area of cross-section.

		Spacecraft area of cross-section		
		Minimum	Average	Maximum
Lifetime (days)	Solar minimum	85	40	30
	Solar mean	42	20	15
	Solar maximum	24	12	8

It is evident from Figs. 2-4 that the time to decay is extremely sensitive to the spacecraft's area of cross-section and may vary between 24 days and 8 days during solar maximum. Additionally, it can also be seen that for all three cases of solar flux, the ratio between the different lifetimes due to variations in spacecraft area is almost constant.

Solar Cycle

The influence of solar cycle on mission lifetime is seen in Figure 5. Together with the trend of the solar cycle shown in Figure 6, it can be seen that a launch date around 2013 hovers around the solar maximum. This would imply a short lifetime for the mission – 24, 12, and 8 days for maximum, mean and minimum spacecraft area of cross-sections respectively.

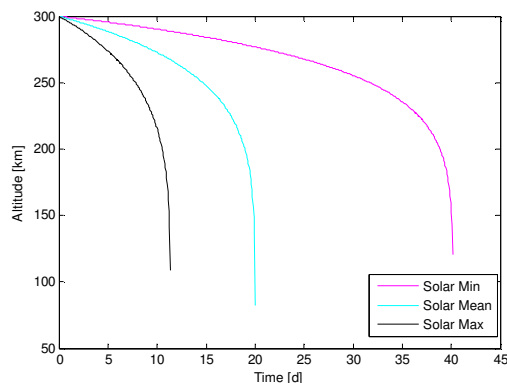


Figure 5: Influence of Solar cycle on lifetime of the satellites. Spacecraft average area of cross-section = 0.021 m²

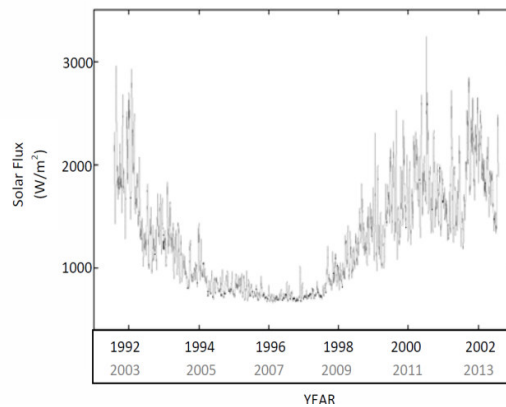


Figure 6: Solar Activity Level between 1992 and 2003¹⁰. With a 11-year solar cycle, the solar activity level is expected to be similar for the next cycle (2003 to 2014).

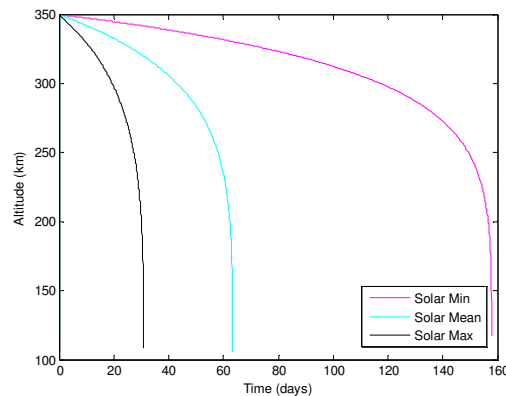


Figure 7: Orbital decay of the satellites with an initial altitude of 350 km. Spacecraft average area of cross-section = 0.021 m²

Further simulations show that an initial altitude of about 350 km is necessary to guarantee a one month lifetime for a launch date of 2013 as shown in Figure 7. The initial altitude has to be raised further for higher expected lifetimes.

Deployment Mechanism

The deployment mechanism provides incremental velocities to the satellites with respect to the reference satellite. To investigate the influence of this incremental velocity on lifetime, the satellite orbits have been numerically propagated with initial velocity increments of 5 m/s along six different directions (positive and negative along-track, cross-track and radial directions with respect to the reference satellite).

The cross-track velocity increment does not change the energy of the orbit, and therefore, upon neglecting small spatial variation of atmospheric drag, does not have an influence on satellite lifetime. The radial velocity increment changes the eccentricity of the orbit with the semi-major axis remaining constant. The change in lifetime is less than one day for a 5 m/s velocity increment in radial direction. The along-track velocity increment changes the semi-major axis and the eccentricity of the orbit. The influence is dominated by the change in semi-major axis, and the lifetime of the satellites increase by 5 days and decrease by 5 days respectively, for a positive and negative velocity increment of 5 m/s along the track.

RELATIVE MOTION BETWEEN THE SATELLITES

In this section the relative motion between the QB50 spacecraft will be analyzed and characterized. To start with, we limit ourselves to non-perturbed orbits and perform a qualitative analysis of the relative motion of the satellites stemming from the initial velocity increments provided by the deployment mechanism. The initial relative velocity vectors determine the evolving cluster configuration. The results allow a first assessment of the evolving relative geometry within the cluster. This is followed by a treatment of the relative motion including the effects of drag and the aspherical Earth's gravity field.

A satellite in LEO experiences significant disturbances from atmospheric drag, solar radiation pressure, the complex Earth's gravity field, luni-solar perturbations and other effects¹¹. For satellites at 300 km altitude, the two major perturbations are atmospheric drag and the higher order terms in the harmonic expansion of the Earth's gravity field. Only these two effects will be addressed in the sequel. For all analysis in this study the inertial states of the satellite orbits are propagated to compute the relative inertial states which are then projected onto the commoving Hill frame.

Relative motion without perturbations

The satellite orbits are initially simulated with no perturbations, corresponding to simple Keplerian orbits. This simplified treatment allows an approximated quantitative and qualitative assessment of the relative motion between the satellites that is caused by the velocity increments from the separation mechanism.

The relative motion between spacecraft has been extensively studied for spacecraft located close to each other using the Hill's equations or the Clohessy-Wiltshire equations¹². With r, ϕ and z representing the motion in the radial, along-track and cross-track

directions as shown in Figure 7, Equation(1) describes the motion in the Hill's frame⁸. Table 4 gives the numerical values for the amplitude and offset of the relative motion for a velocity increment of 1 m/s from the separation mechanism.

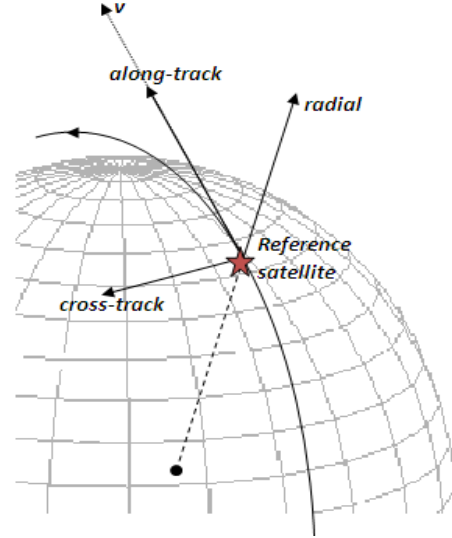


Figure 8: The Hill's reference frame showing along-track, cross-track and radial directions with respect to the reference satellite

$$\begin{aligned}
 r &= -A \cos(nt + \alpha) + 2\left(\frac{\dot{\phi}_0}{n} + 2r_0\right) \\
 \phi &= 2A \sin(nt + \alpha) + \left(\frac{\dot{\phi}_0 - 2\dot{r}_0}{n}\right) \\
 &\quad - 3\left(\dot{\phi}_0 + 2\dot{n}r_0\right)t \\
 z &= A_z \sin(nt + \alpha_z)
 \end{aligned} \tag{1}$$

where,

$$A = \sqrt{\left(\frac{\dot{r}_0}{n}\right)^2 + \left(\frac{2\dot{\phi}_0}{n} + 3r_0\right)^2}$$

$$\alpha = \text{atan}\left(\frac{\dot{r}_0}{2\dot{\phi}_0 + 3r_0 n}\right)$$

$$A_z = \sqrt{z_0^2 + \left(\frac{\dot{z}_0}{n}\right)^2}$$

$$\alpha_z = \text{atan}\left(\frac{n z_0}{\dot{z}_0}\right)$$

Table 4: The amplitude and offset of the relative motion between the satellites for a velocity increment of 1m/s

Velocity increment(1 m/s)		+ along-track	- along-track	+ radial	- radial	+cross-track	- cross-track	
Orbital Element affected		a, e	a, e	e	e	i, Ω	i, Ω	
Along-track	Periodic	Amp. (m)	3457	-3457	1729	-1729	-	-
		Freq.	Orbital period	Orbital period	Orbital period	Orbital period	-	-
	Offset (m)		864	-864	-1729	+1729	-	-
	Secular (m)		-3t	+3t	-	-	-	-
Cross-track	Periodic	Amp. (m)	-	-	-	-	864	-864
		Freq.	-	-	-	-	Orbital period	Orbital period
	Offset		-	-	-	-	-	-
Radial	Periodic	Amp. (m)	-1729	1729	-864	+864	-	-
		Freq.	Orbital period	Orbital period	Orbital period	Orbital period	-	-
	Offset (m)		1729	-1729	-	-	-	-
	Secular (m)		*	*	-	-	-	-

It can be seen from Eq. 2 that along-track, radial and cross-track velocity increments result in a periodic motion around the reference satellite. However, it is only the along-track velocity increment that results in a secular drift leading to a growing satellite separation with time. The periodic relative motion in radial and along-track directions due to a radial velocity increment of ± 1 m/s by the cluster launch mechanism can be seen in Figures 9 and 10.

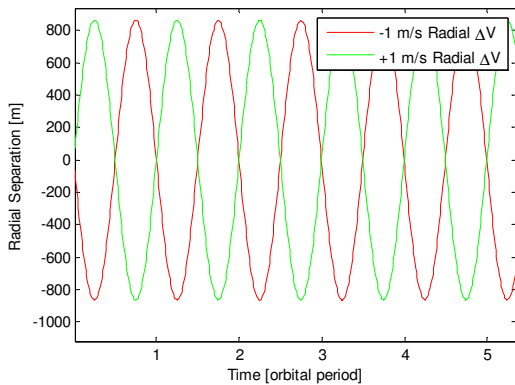


Figure 9: Radial separation with respect to reference arising due to 1 m/s radial velocity increment from the deployment mechanism.

The cross-track motion due to an initial velocity increment of ± 1 m/s in cross-track direction by the cluster launch mechanism is shown in Figure 11. The secular trend in along-track motion resulting from an initial along-track velocity increment of ± 1 m/s and ± 5 m/s is shown in Figure 12. Note that the along-track separation is shown in degrees which accounts for the discontinuity when the separation reaches 360 degrees and then starts from zero. It can be seen that a 5 m/s velocity increment can lead to an along-track separation of approximately half an orbit in 15 days.

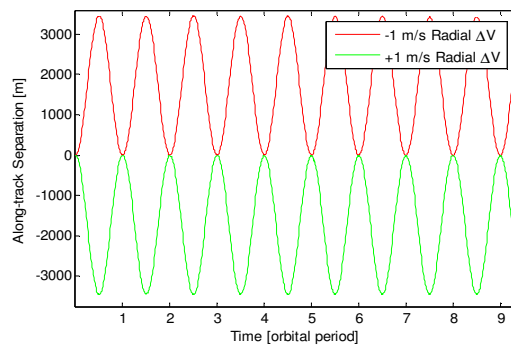


Figure 10: Along-track separation with respect to reference arising due to 1 m/s radial velocity increment from the deployment mechanism.

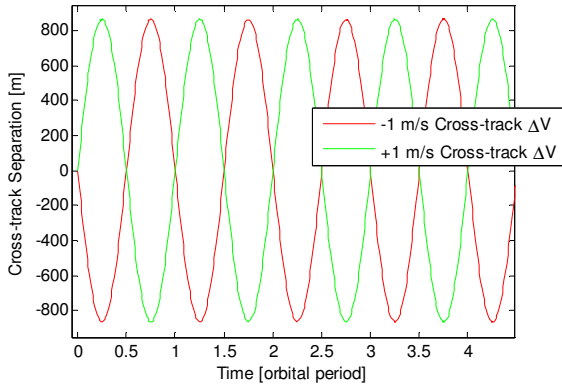


Figure 11 Cross-track separation with respect to reference arising due to 1 m/s cross-track velocity increment from the deployment mechanism.

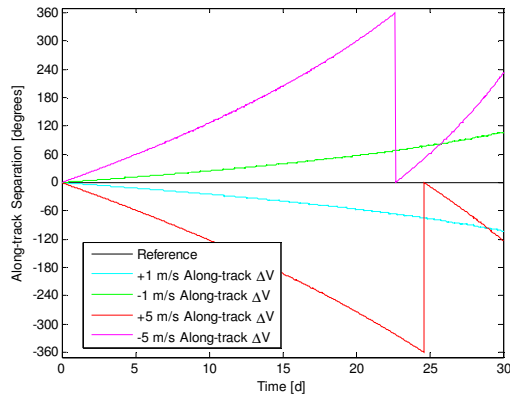


Figure 12: Along-track separation with respect to reference arising due to 1 m/s and 5 m/s along-track velocity increments from the deployment mechanism.

Differential Drag

Atmospheric drag plays a significant role in the orbit evolution of low earth orbiting satellites. When there are multiple satellites, the drag experienced by each can be different even when they are orbiting at the same altitude and relatively close to each other. This gives rise to differential drag, which can significantly influence the relative motion between satellites. Differential drag is caused by differences in the individual spacecraft masses and cross-sectional area, local density variations and differences in the drag coefficient of the two spacecraft¹⁴. Drag acts opposite to the satellite velocity vector and decreases the energy of

the orbit and the effect of differential drag always manifest as a growing along-track separation. Figure 13 shows the along-track separation resulting from a differential drag of 10%. It can be seen that in around 30 days, the satellite suffering more drag has moved approximately a quarter of an orbit ahead of the reference satellite.

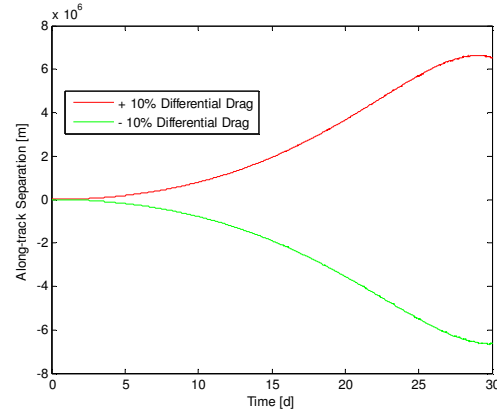


Figure 13: Along-track separation with respect to reference due to differential drag of 10%.

Assuming circular orbits, a simplified expression for the change in semi-major axis due to drag over one orbit is given in Equation (2)⁹

$$\Delta a = -2\pi \left(\frac{C_D A}{m} \right) \rho a^2 \quad (2)$$

Where A is the area of the satellite normal to the velocity vector, m is the mass of the satellite, C_D is the ballistic coefficient, and ρ is the density of the atmosphere at a given semi-major axis a . $\delta\Delta a$ is defined as

$$\delta\Delta a = \Delta a_2 - \Delta a_1 \quad (3)$$

Δa_1 and Δa_2 represent the decay in semi-major axis of the two satellites with differential drag over the entire duration under consideration. The total along-track separation because of the differential orbit decay stemming from the differential drag can now be expressed as in Equation (4).

$$AT_{diff.drag} = 3\pi \delta\Delta a * (no. of orbits) \quad (4)$$

Equation (4), can also be used to determine the $\delta\Delta$ required to counter the along-track separation due to differential drag.

Differential Gravity

To analyze the influence of differential gravity on the relative motion, the satellite orbits have been numerically propagated using the Earth's gravitational field up to degree and order 20 of the harmonic expansion. The representation of the resulting relative motion in Hill's frame is not very useful to gain insight into the evolution of the relative motion in the presence of gravity perturbations. More appropriate representations are possible using representations based on e/i -vectors^{7,14} and relative inclination - relative phase⁸. In this paper we do not elaborate on these representations further, but conclude with a qualitative analysis.

The effect of the differential gravity effects due to the higher harmonics in the gravity field can be analyzed by investigating the difference in orbital elements. Initial velocity increments in along-track direction changes the semi-major axis a and eccentricity e of the orbit and velocity increments in radial direction change only e . The change in e causes a differential rotation rate for the argument of perigee.

Satellites subjected to a cross-track velocity increment show either an inclination difference with respect to the reference or a difference in the right ascension of ascending depending upon the position in the orbit where the velocity increment was instantiated. A velocity increment at the equator will cause the inclination to change while a ΔV at the poles will shift the right ascension of ascending node.

ORBIT CONTROL WITH MICROPROPULSION

The possibility of using the TUDelft satellites equipped with micro-propulsion for drag compensation and differential drag compensation will be assessed in this section. Orbit control, if possible, can lead to enhanced lifetime of the mission, stable observation conditions, controlled spatial and temporal resolution, enhanced ground communication, and in general other benefits that an uncontrolled spacecraft cannot provide. Relative orbit control in particular through differential drag compensation can result in stable and controlled along-track separation that can enhance the science return of the mission.

Absolute Orbit Control

Absolute orbit control will be limited to the treatment of compensating orbit decay due to atmospheric drag. The ΔV required to maintain the satellite within an altitude band of 280 to 300 km for 2 months is estimated for different conditions of solar flux. Impulsive ΔV s are assumed to perform orbit raising maneuvers to obtain an approximate estimate of the thrust and fuel requirements. The orbit is allowed to decay up to 280 km before a maneuver is initiated to raise the orbit. The fuel required is estimated by using the basic Tsiolkovsky equation and assuming a specific impulse of 60 s.

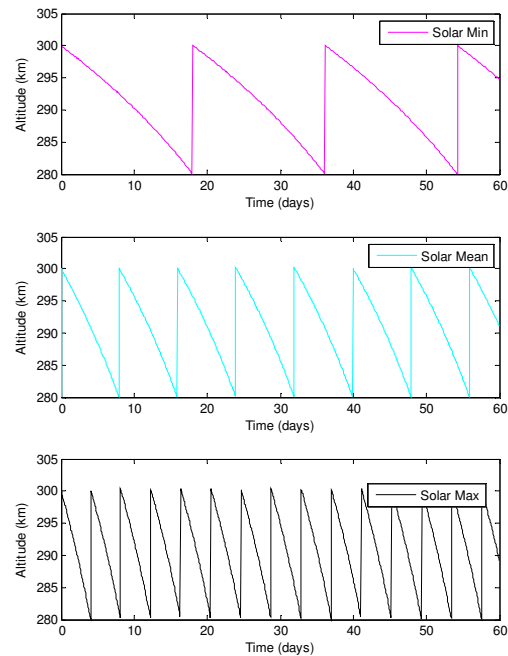


Figure 14: Orbit raising maneuvers under different conditions of solar activity. Spacecraft average area of cross-section = 0.021 m²

Table 5: ΔV maneuvers and fuel required for absolute orbit maintenance between 280 and 300 km

	No. of maneuvers	ΔV per maneuver (m/s)	Total ΔV (m/s)	Fuel required (g)
Solar min	3	11.6	34.8	115
Solar mean	7	11.6	81.2	258
Solar max	14	11.6	162.4	483

For the assumption of impulsive ΔV , the ΔV requirements shown in Table 5 will not be affected by a change in the altitude band gap (20 km between 280 and 300 km altitude). However this band gap drives the requirement on thrust levels and thrust duration of the propulsion system. For example, a 40 mN cold gas thruster will have to operate for around 575 s, to provide the required ΔV of 11.6 m/s per maneuver (ignoring gravity loss, which increases with increased duration of thrusting). The thrusting duration can be reduced by reducing the band gap and increasing the frequency of maneuvers. A shorter band gap will also lead to lesser ΔV as the orbital decay rate due to drag is lower at higher altitudes.

Relative Orbit Control

Relative orbit control will be limited to the treatment of differential drag induced along-track separation. Differential drag can significantly influence the along-track separation between two spacecraft as explained before. Differential drag may be modeled as differential acceleration Δa_D according to Equation (5)³

$$\Delta a_D \approx \frac{1}{2} \left(\frac{C_{D1} A_1}{m_1} \rho(r_1) - \frac{C_{D2} A_2}{m_2} \rho(r_2) \right) v^2 \quad (5)$$

where $\rho(r)$ denotes the atmospheric density at position r and v the spacecraft velocity with respect to the atmosphere. To represent a 10% difference in the differential drag, we can assume equal Area-to-mass ratios and since both spacecraft are relatively close to each other, equal densities and velocities, and establish Equation (6).

$$\begin{aligned} \Delta a_{D_{10\%}} &\approx \frac{1}{2} \left(\frac{A}{m} \rho v^2 \right) (C_{D2} - C_{D1}) \\ &\approx \frac{1}{2} \left(\frac{A}{m} \rho v^2 \right) (0.1 \times 2.2) \end{aligned} \quad (6)$$

where C_{D2} is 1.1 times C_{D1} and $C_{D1} = 2.2$. This results in differential accelerations as shown in Table 6.

Table 6: Differential acceleration due to drag at different height regimes for mean solar flux and average spacecraft cross-section

Height (km)	Density (Kg/m ³)	Δa_D (m/s ²)
300	1.95×10^{-11}	1.34×10^{-6}
250	6.24×10^{-11}	4.30×10^{-6}
200	2.53×10^{-10}	1.74×10^{-5}

As can be seen in Table 6, the differential acceleration can vary quite considerable over the height range considered. To continuously compensate for this differential acceleration, ΔV s of 1.5, 0.37, and 0.12 m/s/day is required at heights of 200, 250 and 300 km respectively. Since we have considered continuous compensation, this represents a more optimistic scenario. As can be seen from Table 7, the fuel required for differential drag compensation is quite reasonable, especially in the higher height regime, and therefore differential drag compensation is possible with CubeSats.

Table 7: ΔV and fuel required for differential drag compensation

Δa_D (m/s ²)	ΔV required for continuous compensation of differential drag (m/s/day)	Fuel required (g/day)
1.34×10^{-6}	0.12	0.41
4.30×10^{-6}	0.37	1.26
1.74×10^{-5}	1.5	5.1

CONCLUSIONS

The relative motion of a cluster of nano-satellites launched by a single rocket and separated by a deployment mechanism in low earth orbit has been characterized and analyzed. It has been shown that with an initially proposed orbital altitude of 300 km and a launch date in 2013, the proposed QB50 mission lifetime of 3 months cannot be met. Further simulations have shown that an initial altitude of about 350 km is

necessary to guarantee a more reasonable lifetime with the same launch date.

Several concluding remarks can be made from the investigation of the orbital evolution of the QB50 satellite cluster. The velocity increments from the separation mechanism can be directly linked to the trend in the orbital evolution of the cluster and varying the velocity increments can lead to a variety of potential configurations. The relative motion is extremely sensitive to along-track velocity increments from the deployment mechanism. A high velocity increment is needed in radial and cross-track directions to inflict significant separations in these directions whereas a small along-track velocity increment can lead to secularly growing separation. This translates to high pointing accuracy of the cluster separation mechanism to achieve specific cluster configurations

Differential drag is the most significant perturbation which can lead to tremendous along-track separations within a short span of time. The implications are evident for 2-unit CubeSats, considered in this study as part of the QB50 network, which can have significant variations in the exposed cross-sectional area.

The possibility of micro-propulsion in the two TUDelft CubeSats for drag compensation and differential drag compensation has been investigated. Drag compensation for absolute orbit control stretches the upper achievable limit with a CubeSat even in optimistic conditions of solar flux. It would be technologically and operationally very demanding to demonstrate drag compensation with an active 2 kg CubeSat within the QB50 network. As the results have indicated, relative orbit control through differential drag compensation is a valid proposition and a very useful technology demonstration objective in itself. Differential drag compensation will allow the possibility of a controllable baseline between sensors situated on different spacecraft. This can enhance the science return and provide unique benefits within the QB50 space network.

REFERENCES

1. Sabol, Chris, Burns, Rich and A., McLaughlin Craig. *Satellite Formation Flying Design and Evolution*. 2001, Vol. 38, 2.
2. Gill, E. *Together in Space – Potentials and Challenges of Distributed Space Systems; Inaugural speech; Delft University of Technology (2008)*. .
3. E. Gill, P. Sundaramoorthy, J. Bouwmeester, B. Sanders. *Formation Flying to Enhance the QB50 Space Network*. THE 4S SYMPOSIUM, Funchal, Madeira, 2010.
4. Muylaert, J., et al., *QB50: An International Network of 50 Cubesats for Multi-Point, In-Situ Measurements in the Lower Thermosphere and for Re-Entry Research*. ESA Atmospheric Science Conference, Barcelona, Spain, 7-11 September 2009.
5. P.P., Sundaramoorthy, et al., et al. *Preliminary Orbit Analysis of the QB50 Satellite Cluster*. 4th International Conference on Astrodynamics Tools and Techniques, Madrid, Spain, 2010.
6. Nason, I, Puig-Suari, J and Twiggs, R., *Development of a family of picosatellite deployers based on the CubeSat standard*. Proceedings of the 2002 IEEE Aerospace Conference, Big Sky, MT, Vol. 1, 2000.
7. Montenbruck, Oliver and D'Amico, Simone. *Proximity operations of formation-flying spacecraft using an eccentricity/inclination vector separation*. Journal of Guidance, Control, and Dynamics. Vol. 29, No. 3, 2006.
8. Wertz, J.R. *Mission Geometry; Orbit and Constellation Design and Management*. Kluwer Academic; pp. 510 - 521, 2001. Kluwer Academic; pp. 527 - 533, 2001.
9. Wertz, J.R. *Mission Geometry; Orbit and Constellation Design and Management*. Kluwer Academic; pp. 68 - 74, 2001.
10. Ijssel, Jose Van Den and P.N.A.M, Visser. *Swarm End-to-end Simulator*. Delft : s.n., 2004. CCN2 - EOP -SM/1000/ls.:1-2.
11. Montenbruck, Oliver and Gill, Eberhard. *Satellite Orbits - Models Methods Applications*. s.l. : Springer, 2000. ISBN 3-540-67280-X.
12. Clohessy, W.H., and Wiltshire, R.S. *Terminal Guidance for Satellite Rendezvous*. J. Aerospace Sciences, Vol 27 (1960), p 653.
13. Gill, Eberhard and Runge, Hartmut. *Tight formation flying for an along-track SAR interferometer*. Acta Astronautica, Vol 55, Issue 3, 2004.
14. P.P. Sundaramoorthy, E. Gill, C.J.M. Verhoeven. *Relative Orbital Evolution of a Cluster of Femto-Satellites in Low Earth Orbit*. Space Flight Mechanics Meeting, CA, USA, 2010.
15. Bate, Mueller and White. *Fundamentals of Astrodynamics*. s.l. : Dover, 1971. ISBN 0-486-60061-0.